Journal of
Materials Chemistry

Cite this: *J. Mater. Chem.*, 2012, **22**, 19673

www.rsc.org/materials

PAPER

Functional heterometallic coordination polymers with metalloligands as tunable luminescent crystalline materials†

Dong-Ying Du,[a] Jun-Sheng Qin,[a] Cheng-Xin Sun,[b] Xin-Long Wang,*[a] Shu-Ran Zhang,[a] Ping Shen,[a] Shun-Li Li,[a] Zhong-Min Su*[a] and Ya-Qian Lan*[a]

Received 15th May 2012, Accepted 30th July 2012
DOI: 10.1039/c2jm34661c

Five heterometallic luminescent crystalline materials with the metalloligand, $[Zn(HL)Eu_xTb_y(H_2O)_2][ZnBr_4]\cdot H_2O$ ($x = 1$, $y = 0$, **IFMC-21**; $x = 0.75$, $y = 0.25$, **IFMC-22**; $x = 0.5$, $y = 0.5$, **IFMC-23**; $x = 0.25$, $y = 0.75$, **IFMC-24**; $x = 0$, $y = 1$, **IFMC-25**; H_4L = 4,4′,4″,4‴-(2,2′,2″,2‴-(ethane-1,2-diylbis(azanetriyl))tetrakis(methylene)-tetrakis-(1*H*-benzo[*d*]imidazole-2,1-diyl))tetrakis(methylene)-tetrabenzoic acid; IFMC = Institute of Functional Material Chemistry), were prepared by the combination of hydrothermal and ionothermal methods for the first time. **IFMC-21–25** can be obtained by introducing the desired Eu(III) and Tb(III) in the initial experiments. In these crystalline materials, the metalloligand Zn(HL) was connected by bi-lanthanide cores leading to a 2D sheet-structure and $[ZnBr_4]^{2-}$ ions were distributed in the interspaces of the sheet. The luminescent properties of **IFMC-21** to **25** were investigated and the results reveal that they exhibit characteristic Eu(III) and Tb(III) ion emissions, and the intensities of red and green arising from Eu(III) and Tb(III) emissions are shifted correspondingly by tuning the ratios of Eu(III) : Tb(III).

Introduction

The exploratory preparation and investigation of coordination polymers (CPs) and other metal-containing polymers have captured increasing attention in the last decades, driven largely by their functional applications in gas storage, fluorescence, separations, sensors and catalysis.[1–4] Lanthanide (Ln)-CPs are especially attractive due to their versatile coordination geometries and unique luminescent properties; the organic linker can serve as an antenna that sensitizes the lanthanide emission, which is extensively utilized in optoelectronics, display devices and up-conversion phosphors.[5] Furthermore, materials emitting multiple colors under single-wavelength excitation are of great importance in the area of light display, lasers, and optoelectronic devices. The emission properties of the different individual Ln-based compounds are well documented;[6] however, color modulation in Ln-based CPs by varying the dopant concentration and changing the excitation wavelengths is less explored.[7] Immobilization of functional sites within CPs is very important for their functional properties. The metalloligand approach enables chemists to rationally immobilize a variety of different functional sites such as open metal sites, catalytic active metal sites, photoactive metal sites, and pores of tunable sizes into CPs. The obtained materials have great potential applications in gas storage and separation, sensing, heterogeneous asymmetric catalysis, photoactive and nanoscale drug delivery, and biomedical imaging. The metalloligand approach turns out to be a promising strategy to improve and fine-tune physical and chemical properties of CPs.[8]

Ionic liquids, a class of salts which are liquid at low temperature and consist of ions only, have received considerable attention recently due to their low melting points, high boiling points, low vapor pressure, nonflammability and high thermal stability.[9,10] Ionothermal synthesis, that is, the use of an ionic liquid as solvent and sometimes structure directing agent in the preparation of crystalline solids, has opened up a new way for the creation of novel inorganic and metal–organic compounds.[11] It is undeniable that ionic liquids have certain potential advantages in synthetic chemistry owing to their high solubility for organic, inorganic and organometallic compounds, however, there is no report on the preparation of heterometallic fluorescent CPs with metalloligand *via* the combination of hydrothermal and ionothermal method up to now.

Tetrapodands have been employed to obtain metalloligands in both coordination chemistry and materials chemistry for a long time, typically, *N*,*N*,*N*′,*N*′-tetrakis(2′-benzimidazolyl methyl)-1,2-ethanediamine[12] and its derivatives with different substituent groups on the benzimidazole ring. However, the construction of high dimensional CPs has not been fully realized by employing

---

[a] *Institute of Functional Material Chemistry, Faculty of Chemistry, Northeast Normal University, Changchun 130024, P. R. China. E-mail: zmsu@nenu.edu.cn; lanyq176@nenu.edu.cn; Fax: +86-431-85684009*
[b] *School of Life Sciences, Northeast Normal University, Changchun 130024, P. R. China*

† Electronic supplementary information (ESI) available: additional figures, XRPD, IR spectra and details of crystallographic data. CCDC 879886–879890. For ESI and crystallographic data in CIF or other electronic format. see DOI: 10.1039/c2jm34661c

these ligands due to the cage-like, box-like or capsule-like coordination modes preventing expansion of the frameworks, and their poor solubility in water. Earlier reports indicate that strong interactions exist between water molecules and the anions of ionic liquids.[13] Recent work by Morris and Tian *et al.*,[14] described the positive effect of small amounts of water added to eutectic mixture systems in the ionothermal synthesis of zeolite. These observations inspired us to introduce ionic liquids to a water system in order to improve the synthetic conditions. As our continuing work on 4,4′,4′′,4′′′-(2,2′,2′′,2′′′-(ethane-1,2-diylbis-(azanetriyl))tetrakis(methylene)tetrakis-(1*H*-benzo-[*d*]imidazole-2,1-diyl))tetrakis(methylene)-tetrabenzoic acid (H_4L, Scheme 1),[15] we investigated the reaction of H_4L with $Zn(NO_3)_2$ and lanthanide nitrates by a combination of hydrothermal and ionothermal methods. Fortunately, a family of Ln-based crystalline materials, $[Zn(HL)Eu_xTb_y(H_2O)_2][ZnBr_4]\cdot H_2O$ ($x = 1$, $y = 0$, **IFMC-21**; $x = 0.75$, $y = 0.25$, **IFMC-22**; $x = 0.5$, $y = 0.5$, **IFMC-23**; $x = 0.25$, $y = 0.75$, **IFMC-24**; $x = 0$, $y = 1$, **IFMC-25**, and IFMC = Institute of Functional Material Chemistry), with metalloligands have been successfully synthesized due to the similar nature of Eu(III) and Tb(III) ions. This is the first report on the synthesis of heterometallic materials by the combination of hydrothermal and ionothermal methods. Taking into account the excellent luminescent properties of Eu(III) and Tb(III) ions, the luminescence studies of **IFMC-21–25** were carried out in the solid state at room temperature. The result suggested that they exhibit the characteristic Eu(III) and Tb(III) ions emissions, and the intensities of red and green arising from Eu(III) and Tb(III) emissions will be shifted correspondingly by tuning the ratios of Eu(III):Tb(III).

Results and discussion

Syntheses

The ionic liquid plays an important role in the successful preparation of **IFMC-21–25**. When BMIB (1-butyl-3-methyl-1*H*-imidazol-3-ium bromide) was introduced into this system, the final crystalline products were synthesized in good qualities and moderate yields (Fig. S1a†). The XRPD patterns for **IFMC-21–25** are presented in Fig. S2.† The diffraction peaks of both simulated and experimental patterns match well in key positions, thus indicating their phase purities. While, no crystalline phase was formed if no BMIB was added (Fig. S1b and S2f†). BMIB perhaps serves as a mineralizing agent and increases the solubility of H_4L ligand during the reaction process.

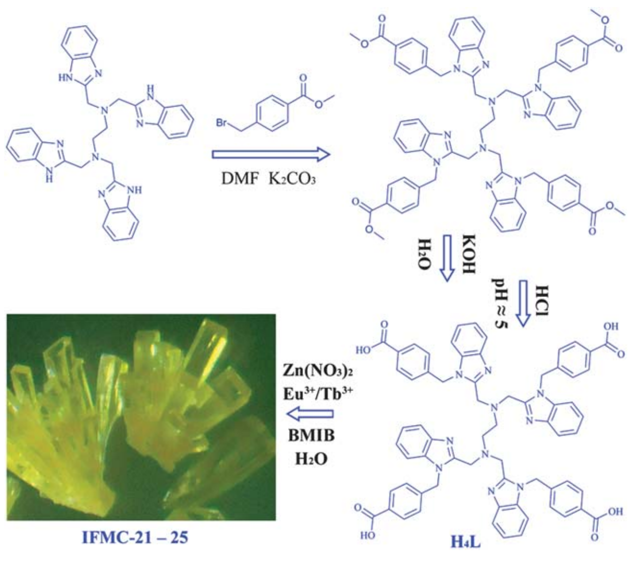

Scheme 1 Preparation of H_4L and **IFMC-21–25**.

Structures of IFMC-21–25

IFMC-21–25 were synthesized from an aqueous mixture of $Zn(NO_3)_2\cdot 6H_2O$, H_4L, $Ln(NO_3)_3\cdot 6H_2O$, and BMIB at 170 °C for 3 days. X-Ray diffraction analysis (please see ESI)† reveals that **IFMC-21–25** crystallize in the monoclinic space group $P2_1/n$ (Table S1†) and are isostructural only with slight differences in bond lengths and bond angles. Therefore, only the structure of **IFMC-21** is described in detail. There are two Zn sites, one Eu ion, one HL^{3-} ligand, four Br^- ions and three water molecules in the crystallographically independent unit. The Zn1 atom is octahedrally coordinated by six nitrogen atoms from one bridging HL^{3-} ligand (Zn–N, 2.076–2.287 Å, Table S2†) to form a metalloligand unit (Fig. 1a). The Zn2 atom is completed by four Br^- ions to give rise to a $[ZnBr_4]^{2-}$ unit (Fig. S3†). Eu1 is nine-coordinated by seven carboxylate oxygen atoms from five H_4L ligands and two water molecules (Eu–O, 2.353–2.694 Å; Eu–O1w, 2.465 Å and Eu–O2w, 2.638 Å), thus generating a bi-europium core (Fig. S4†). The Eu–O bond lengths are all within the normal ranges as reported in the literatures.[16] The binding mode of the carboxylate ligand observed in **IFMC-21** is shown in Fig. S5† and the dihedral angles between the benzimidazole rings and the benzene rings are presented in Table S3.† One HL^{3-} anion coordinates to five Eu(III) cations and three bi-europium

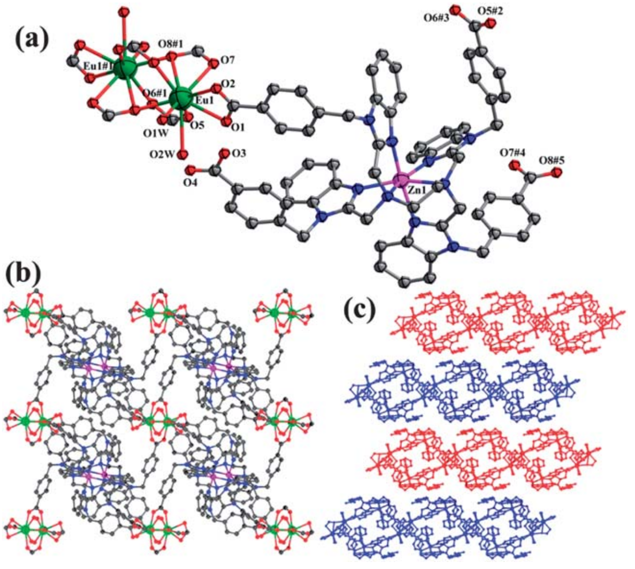

Fig. 1 (a) Coordination environments of the Zn(II) and Eu(III) centres in **IFMC-21**. Symmetry codes: #1: 3 − *x*, −*y*, 1 − *z*; #2: −1 + *x*, *y*, *z*; #3: 2 − *x*, −*y*, 1 − *z*; #4: 2 − *x*, 1 − *y*, 1 − *z*; #5: −1 + *x*, 1 + *y*, *z*. (b) and (c) ball-and-stick representations of the 2D sheet-like structure and its packing arrangement in **IFMC-21**, respectively. All the hydrogen atoms are omitted for clarity.

cores, in turn, one bi-europium core connects six HL^{3-} ions (Fig. S6†). Such connectivity modes give rise to a two-dimensional network in the *ab* plane of **IFMC-21** (Fig. 1b and S7†), which is packed in the *ac* plane as depicted in Fig. 1c. In addition, the $[ZnBr_4]^{2-}$ anions working as counterions are distributed in the interspaces of the sheet-like architecture (Fig. S8†).

Luminescent properties

An absorption spectrum of H_4L in ethanol exhibits an absorption maximum at 292 nm (Fig. S9†), and a broad emission peak centered at 451 nm was observed when excited at 364 nm (Fig. S10†). Upon excitation at 395 nm, **IFMC-21** yields intense red luminescence in the solid state at room temperature and exhibits characteristic peaks at 580, 595, 617, 653, and 701 nm originating from the transitions of $^5D_0 \rightarrow {}^7F_J$ ($J = 0$–4) of the Eu(III) ions (Fig. 2a). A comparison of the luminescence measured at room temperature and low temperature further confirms this assignment (Fig. 2a and S11†). The $^5D_0 \rightarrow {}^7F_4$ transition is clearly stronger monitored at a low temperature than that at room temperature. The appearance of the symmetry-forbidden emission $^5D_0 \rightarrow {}^7F_0$ at 580 nm indicates that Eu(III) ions in **IFMC-21** occupy sites with low symmetry.[16] The $^5D_0 \rightarrow {}^7F_2$ transition is clearly stronger than the $^5D_0 \rightarrow {}^7F_1$ transition with an intensity ratio of about 3.3 for $I(^5D_0 \rightarrow {}^7F_2)/I(^5D_0 \rightarrow {}^7F_1)$, indicating the absence of inversion symmetry at the Eu^{3+} site, which is in agreement with the result of single crystal X-ray analysis.[17] Furthermore, it is clear to see that **IFMC-21** forms a highly transparent block solid under optical microscopy and exhibits a red color when excited with UV light of 365 nm (Fig. S12a and b†).

IFMC-25 yields an intense green luminescence when excited at 365 nm, which is assigned to the characteristic transitions of $^5D_4 \rightarrow {}^7F_J$ ($J = 3$–6) of the Tb(III) ions (Fig. 2b). Two intense emission bands at 492 and 545 nm correspond to $^5D_4 \rightarrow {}^7F_6$ and $^5D_4 \rightarrow {}^7F_5$ while the weaker emission bands at 584 and 622 nm originate from $^5D_4 \rightarrow {}^7F_4$ and $^5D_4 \rightarrow {}^7F_3$.[18] Moreover, there is no obvious variation between luminescent spectra measured at room temperature and low temperature. Similarly, the pictures were taken under optical microscopy (Fig. S12c and d†).

Owing to the promising luminescent sensors with Eu(III) and Tb(III) ions, we tried to make them cocrystallize with tunable optical activity. Fortunately, $[ZnEu_xTb_y(HL)(H_2O)_2][ZnBr_4]\cdot H_2O$ ($x = 0.75$, $y = 0.25$, **IFMC-22**; $x = 0.5$, $y = 0.5$, **IFMC-23**; $x = 0.25$, $y = 0.75$, **IFMC-24**) were successfully prepared. Meanwhile, the emission and excitation spectra were also recorded under similar conditions (Fig. 3). **IFMC-21–25** exhibit large broad blue-shift emission bands with a relatively weak intensity in the range of 350–450 nm with respect to free H_4L, which can be assigned to the emission of ligand H_4L.[19] The occurrence of the ligand-based emission in the fluorescence spectra of metal complexes reveals that the energy transfer from the ligand to the metal centre is ineffective and cannot sensitise the metal emission to a large extent. Further experiments using a fluorescence microscope equipped with a CCD camera to demonstrate the luminescent behaviours were carried out. With tuning the ratios of Eu(III) : Tb(III), the intensities of red and

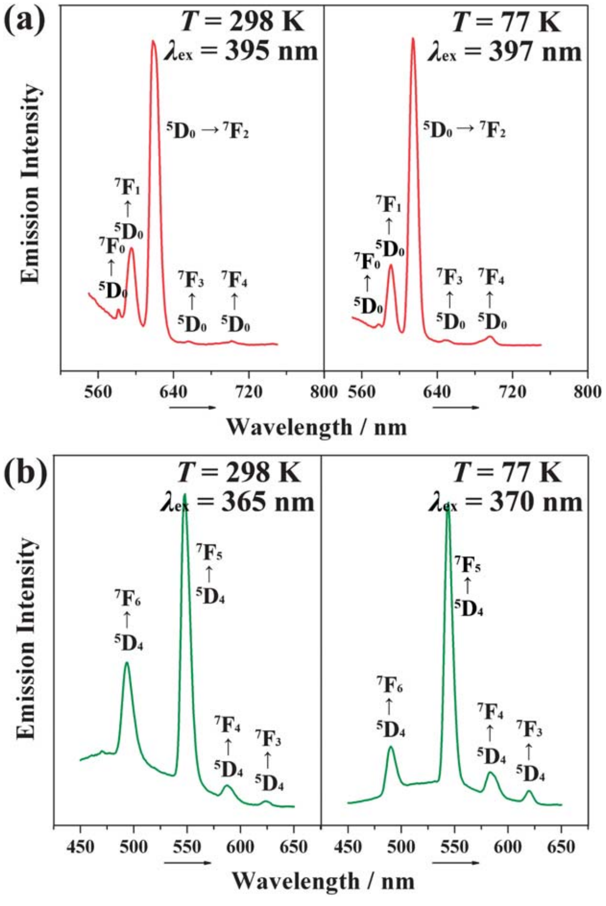

Fig. 2 Emission spectra of **IFMC-21** (a) and **IFMC-25** (b).

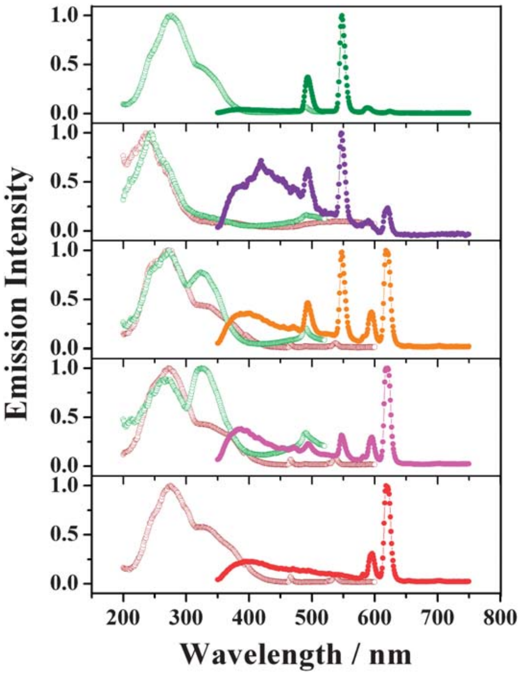

Fig. 3 Emission spectra (●, $\lambda_{ex} = 276$ nm) and excitation spectra (○, wine: $\lambda_{em} = 619$ nm; green, $\lambda_{em} = 548$ nm) of **IFMC-21–25** (down → top) in the solid state at room temperature.

green arising from Eu(III) and Tb(III) emissions will be shifted correspondingly. The encouraging result suggests that multicolor emission ranging from red to green can be realized within the Eu_xTb_y-based MOFs by tuning the ratios of Eu(III):Tb(III) (Fig. S13†).[20]

The decay curve of $^5D_0 \rightarrow {}^7F_2$ transition (617 nm) for **IFMC-21** (Fig. S14a†) is well-fitted by an exponential function, yielding the lifetime value of $\tau = 0.48$ ms. Similarly, for **IFMC-25**, the decay curve of $^5D_4 \rightarrow {}^7F_5$ transitions (545 nm) is well-fitted by an exponential function, yielding a lifetime value of 0.97 ms (Fig. S14b†). Furthermore, both the Eu(III) and Tb(III) decay curves in **IFMC-22–24** were also investigated. Fig. S14a† shows the Eu(III) decay curves detected at $^5D_0 \rightarrow {}^7F_2$ transitions (617 nm) of **IFMC-22–24**, which are well-fitted by exponential functions with lifetime values of $\tau = 0.52$, 0.50 and 0.60 ms, respectively. Meanwhile, the Tb(III) decay curves monitored at $^5D_4 \rightarrow {}^7F_5$ transitions (545 nm) of **IFMC-22–24**, which are well-fitted by exponential functions (Fig. S14b†), yielding lifetime values of $\tau = 0.88$, 0.84 and 0.88 ms, respectively. The changes in lifetime of different lanthanide ions in **IFMC-21–25** is perhaps caused by their environments and the error in the lifetime measurement. This result reveals that there is no energy-transfer occurred in **IFMC-22–24**.[21] In addition, the quantum yields of **IFMC-21–25** are presented in Table 1.

Experimental

Materials and measurements

The starting material H_4L was synthesized according to the procedure described in the literature with some modifications[15] and characterized by elemental analysis, UV (Fig. S9†), luminescence (Fig. S10†) and ^1H NMR spectra (Fig. S15†). All other chemicals were obtained from commercial sources and were used without further purification. Elemental analyses (C, H and N) were performed on a Perkin-Elmer 240C elemental analyzer, Eu and Tb were determined with ICP-OES Spectrometer (USA). IR spectra were recorded in the range 4000–400 cm^{-1} on an Alpha Centaurt FT/IR spectrophotometer using KBr pellets. X-Ray powder diffraction measurements were performed on a Siemens D5005 diffractometer with Cu-Kα ($\lambda = 1.5418$ Å) radiation in the range of 3–60° at 293 K. UV/Vis spectroscopy was performed with a U-3010 spectrophotometer. ^1H NMR spectrum was measured on Bruker Avance 500 MHz with tetramethylsilane as the internal standard. Solid-state fluorescence spectra for **IFMC-21–25** were recorded on a F-7000 FL spectrophotometer equipped with a xenon lamp and quartz carrier at room temperature. The photoluminescent quantum yields of crystalline **IFMC-21–25** (Fig. S1a†) were measured in an integrating sphere (for Eu(III), $\lambda = 276$ nm; for Tb(III), $\lambda = 281$ nm). The excited-state lifetimes were measured by exciting the samples with 355 nm light pulses with ~5 ns pulse width from a Quanty-Ray DCR-2 pulsed Nd:YAG laser.

X-Ray crystallography

Single crystal X-ray diffraction data in this work were recorded on a Bruker APEXII CCD diffractometer with graphite-monochromated Mo Kα radiation ($\lambda = 0.71069$ Å) at 293 K. Absorption corrections were applied using multi-scan technique. All the structures were solved by Direct Method of SHELXS-97 (ref. 22*a*) and refined by full-matrix least-squares techniques using the SHELXL-97 program[22b] within WINGX.[22c] Hydrogen atoms on the H_4L ligands were placed on calculated positions and included in the refinement riding on their respective parent atoms. Anisotropic thermal parameters were used to refine all non-hydrogen atoms. Those hydrogen atoms attached to lattice water molecules were not located.† The crystal data and structure refinement results of **IFMC-21–25** are summarized in Table S1.† The selected bond lengths of **IFMC-21–25** are listed in Table S2.†

Syntheses of IFMC-21–25

These compounds were prepared using an analogous method. In typical experiments, **IFMC-21–25** were prepared as follows: $Zn(NO_3)_2 \cdot 6H_2O$ (0.10 g, 0.34 mmol), H_4L (0.10 g, 0.089 mmol) and BMIB (0.40 g, 1.83 mmol) were dissolved in distilled water (10 mL) with vigorous stirring for 20 min, and then $Eu(NO_3)_3 \cdot 6H_2O$ or $Tb(NO_3)_3 \cdot 6H_2O$ (0.10 g, 0.23 mmol) was added to the mixture and stirred for another 20 min. The resulting solution was transferred and sealed in a 23 mL Teflon-lined stainless steel container, which was heated at 170 °C for 72 h. After the autoclave was cooled to room temperature at 10 °C h^{-1}, light yellow block crystals suitable for X-ray crystallography were obtained, and then washed with distilled water and air-dried. For **IFMC-22–24**, the Eu(III)/Tb(III) mixed samples were prepared by introducing the desired Eu(III) and Tb(III) contents in the initial experiments. In addition, the contents of Eu(III) and Tb(III) in the final products were presented in Table 1.

$[Zn(HL)Eu(H_2O)_2][ZnBr_4] \cdot H_2O$ (**IFMC-21**). 68% yields (based on H_4L). Elemental analysis: Anal. calc. for $C_{66}H_{59}N_{10}O_{11}Br_4Zn_2Eu$ (1770.57): C 44.77; H 3.36; N 7.91; Zn 7.39; Eu 8.58. Found: C 44.72; H 3.42; N 7.97; Zn 7.35; Eu

Table 1 The elemental contents, excited-state lifetime and quantum yields of Eu(III) and Tb(III) in **IFMC-21–25**

	Elemental contents (%)		The molar ratios of Eu(III):Tb(III)	Lifetime (ms)		Quantum yield (%)	
	Eu(III)	Tb(III)		Eu(III)	Tb(III)	Eu(III)	Tb(III)
IFMC-21	8.50	0	4 : 0	0.48	—UD[a]	4.3	—UD[a]
IFMC-22	6.38	2.19	3.05 : 1	0.52	0.88	3.9	3.4
IFMC-23	4.24	4.38	2.02 : 2	0.50	0.84	3.5	4.6
IFMC-24	2.07	6.78	0.96 : 3	0.60	0.88	1.8	2.7
IFMC-25	0	8.87	0 : 4	—UD[a]	0.97	—UD[a]	4.6

[a] UD: undetected.

8.50%. IR (KBr, cm^{-1}, Fig. S16a†): 3424 (m), 1687 (m), 1613 (s), 1537 (m), 1482 (s), 1453 (s), 1406 (s), 1329 (s), 1288 (w), 1179 (w), 1098 (s), 1012 (w), 921 (m), 889 (m), 860 (w), 744 (s), 713 (m), 638 (w), 563 (w), 426 (w).

$[Zn(HL)Eu_{0.75}Tb_{0.25}(H_2O)_2][ZnBr_4]\cdot H_2O$ (**IFMC-22**). 56% yields (based on H_4L). Elemental analysis: Anal. calc. for $C_{66}H_{59}N_{10}O_{11}Br_4Zn_2Eu_{0.75}Tb_{0.25}$ (1772.31): C, 44.73; H, 3.36; N, 7.90; Zn, 7.38; Eu, 6.43; Tb, 2.24. Found: C 44.80; H 3.41; N 7.96; Zn 7.30; Eu 6.38; Tb 2.19%. IR (KBr, cm^{-1}, Fig. S16b†): 3424 (s), 1688 (m), 1614 (s), 1536 (m), 1482 (s), 1453 (s), 1405 (s), 1328 (s), 1279 (m), 1178 (m), 1095 (m), 1012 (w), 921 (w), 889 (w), 863 (w), 743 (s), 711 (m), 638 (w), 560 (w), 523 (w), 425 (w).

$[Zn(HL)Eu_{0.5}Tb_{0.5}(H_2O)_2][ZnBr_4]\cdot H_2O$ (**IFMC-23**). 63% yields (based on H_4L). Elemental analysis: Anal. calc. for $C_{66}H_{59}N_{10}O_{11}Br_4Zn_2Eu_{0.5}Tb_{0.5}$ (1774.05): C, 44.68; H, 3.35; N, 7.90; Zn, 7.37; Eu, 4.28; Tb, 4.48. Found: C 44.75; H 3.41; N 7.96; Zn 7.32; Eu 4.24; Tb 4.38%. IR (KBr, cm^{-1}, Fig. S16c†): 3424 (s), 1685 (m), 1614 (s), 1535 (m), 1482 (s), 1453 (s), 1406 (s), 1328 (s), 1279 (m), 1177 (m), 1096 (m), 1012 (w), 920 (w), 889 (w), 864 (w), 743 (s), 711 (w), 638 (w), 561 (w), 523 (w), 426 (w).

$[Zn(HL)Eu_{0.25}Tb_{0.75}(H_2O)_2][ZnBr_4]\cdot H_2O$ (**IFMC-24**). 58% yields (based on H_4L). Elemental analysis: Anal. calc. for $C_{66}H_{59}N_{10}O_{11}Br_4Zn_2Eu_{0.25}Tb_{0.75}$ (1775.79): C, 44.64; H, 3.35; N, 7.89; Zn, 7.36; Eu, 2.14; Tb, 6.71. Found: C 44.73; H 3.42; N 7.95; Zn 7.27; Eu 2.07; Tb 6.78%. IR (KBr, cm^{-1}, Fig. S16d†): 3439 (m), 1689 (m), 1614 (s), 1536 (m), 1482 (s), 1453 (s), 1407 (s), 1328 (s), 1279 (m), 1178 (m), 1095 (w), 1012 (w), 921 (w), 889 (w), 864 (w), 743 (s), 712 (m), 639 (w), 561 (w), 523 (w), 426 (w).

$[Zn(HL)Tb(H_2O)_2][ZnBr_4]\cdot H_2O$ (**IFMC-25**). 72% yields (based on H_4L). Elemental analysis: Anal. calc. for $C_{66}H_{59}N_{10}O_{11}Br_4Zn_2Tb$ (1777.53): C 44.60; H 3.35; N 7.88; Zn 7.36; Tb 8.94. Found: C 44.66; H 3.33; N 7.82; Zn 7.32; Tb 8.87%. IR (KBr, cm^{-1}, Fig. S16e†): 3443 (w), 2905 (w), 1691 (w), 1614 (m), 1515 (m), 1481 (m), 1454 (m), 1411 (s), 1329 (m), 1280 (m), 1178 (w), 1097 (m), 1012 (w), 938 (w), 889 (w), 865 (w), 743 (s), 712 (m), 643 (w), 563 (w), 525 (w), 424 (w).

Conclusions

In summary, a series of heterometallic Ln-based luminescent materials with metalloligands have been successfully prepared by the combination of hydrothermal and ionothermal methods for the first time. Crystalline materials, **IFMC-21–25**, were obtained by introducing the desired Eu(III) and Tb(III) contents in the initial experiments. **IFMC-21** and **25** emit characteristic red and green colors of Eu(III) and Tb(III) ions, respectively. In addition, **IFMC-22–24** also exhibit the characteristic Eu(III) and Tb(III) emissions, and multicolor emission ranging from red to green can be realized within the Eu_xTb_y-based CPs by simply tuning their ratios. The present work not only opens new ways in the preparation of heterometallic CPs through the combination of hydrothermal and ionothermal methods, but also provides an example for tuning the luminescence of crystalline materials. More work in this field is currently under way.

Acknowledgements

This work was financially supported by Pre-973 Program (2010CB635114), the National Natural Science Foundation of China (no. 20901014 and 21001020), the Fundamental Research Funds for the Central Universities (no. 10SSXT137).

Notes and references

1 (*a*) H.-L. Jiang, B. Liu, T. Akita, M. Haruta, H. Sakurai and Q. Xu, *J. Am. Chem. Soc.*, 2009, **131**, 11302; (*b*) D. Esken, S. Turner, O. I. Lebedev, G. V. Tendeloo and R. A. Fischer, *Chem. Mater.*, 2010, **22**, 6393; (*c*) Q.-K. Liu, J.-P. Ma and Y.-B. Dong, *Chem. Commun.*, 2011, **47**, 7185; (*d*) Y.-Q. Lan, H.-L. Jiang, S.-L. Li and Q. Xu, *Adv. Mater.*, 2011, **23**, 5015; (*e*) Z.-Y. Gu and X.-P. Yan, *Angew. Chem., Int. Ed.*, 2010, **49**, 1477; (*f*) N. Chang, Z.-Y. Gu and X.-P. Yan, *J. Am. Chem. Soc.*, 2010, **132**, 13645.

2 (*a*) F. Wang, Y.-X. Tan, H. Yang, H.-X. Zhang, Y. Kang and J. Zhang, *Chem. Commun.*, 2011, **47**, 5828; (*b*) H.-L. Jiang, T. Akita, T. Ishida, M. Haruta and Q. Xu, *J. Am. Chem. Soc.*, 2011, **133**, 1304; (*c*) J.-S. Qin, D.-Y. Du, W.-L. Li, J.-P. Zhang, S.-L. Li, Z.-M. Su, X.-L. Wang, Q. Xu, K.-Z. Shao and Y.-Q. Lan, *Chem. Sci.*, 2012, **3**, 2114; (*d*) J. A. Mason, K. Sumida, Z. R. Herm, R. Krishna and J. R. Long, *Energy Environ. Sci.*, 2011, **4**, 3030; (*e*) S. Liu, Z. Xiang, Z. Hu, X. Zheng and D. Cao, *J. Mater. Chem.*, 2011, **21**, 6649; (*f*) Y.-Q. Lan, S.-L. Li, H.-L. Jiang and Q. Xu, *Chem.–Eur. J.*, 2012, **18**, 8076.

3 (*a*) H. L. Jiang and Q. Xu, *Chem. Commun.*, 2011, **47**, 3351; (*b*) K. S. Jeong, Y. B. Go, S. M. Shin, S. J. Lee, J. Kim, O. M. Yaghi and N. Jeong, *Chem. Sci.*, 2011, **2**, 877; (*c*) Y.-Q. Lan, H.-L. Jiang, S.-L. Li and Q. Xu, *Inorg. Chem.*, 2012, **51**, 7484; (*d*) S. R. Caskey, A. G. Wong-Foy and A. J. Matzger, *J. Am. Chem. Soc.*, 2008, **130**, 10870; (*e*) Y. E. Cheon and M. P. Suh, *Chem. Commun.*, 2009, 2296; (*f*) J.-R. Li, R. J. Kuppler and H.-C. Zhou, *Chem. Soc. Rev.*, 2009, **38**, 1477; (*g*) S. R. Venna and M. A. Carreon, *J. Am. Chem. Soc.*, 2010, **132**, 76.

4 (*a*) W.-Y. Wong, *J. Inorg. Organomet. Polym. Mater.*, 2005, **15**, 197; (*b*) W.-Y. Wong, *Dalton Trans.*, 2007, 4495; (*c*) W.-Y. Wong, *Coord. Chem. Rev.*, 2007, **251**, 2400; (*d*) G. R. Whittell and I. Manners, *Adv. Mater.*, 2007, **19**, 3439; (*e*) W.-Y. Wong and C.-L. Ho, *Acc. Chem. Res.*, 2010, **43**, 1246; (*f*) W.-Y. Wong and P. D. Harvey, *Macromol. Rapid Commun.*, 2010, **31**, 671; (*g*) A. S. Abd-El-Aziz, P. O. Shipman, B. N. Boden and W. S. McNeil, *Prog. Polym. Sci.*, 2010, **35**, 714; (*h*) G.-J. Zhou and W.-Y. Wong, *Chem. Soc. Rev.*, 2011, **40**, 2541; (*i*) C.-L. Ho and W.-Y. Wong, *Coord. Chem. Rev.*, 2011, **255**, 2469; (*j*) G. R. Whittell, M. D. Hager, U. S. Schubert and I. Manners, *Nat. Mater.*, 2011, **10**, 176.

5 (*a*) J. Liu and Y. Li, *Adv. Mater.*, 2007, **19**, 1118; (*b*) C. Li, Z. Quan, P. Yang, J. Yang, H. Lian and J. Lin, *J. Mater. Chem.*, 2008, **18**, 1353; (*c*) K. Binnemans, *Chem. Rev.*, 2009, **109**, 4283.

6 (*a*) M. D. Allendorf, C. A. Bauer, R. K. Bhakta and R. J. T. Houk, *Chem. Soc. Rev.*, 2009, **38**, 1330; (*b*) S. Sivakumar, M. L. P. Reddy, A. H. Cowley and R. R. Butorac, *Inorg. Chem.*, 2011, **50**, 4882.

7 (*a*) R. C. Evans, L. D. Carlos, P. Douglas and J. Rocha, *J. Mater. Chem.*, 2008, **18**, 1100; (*b*) K. Liu, H. You, Y. Zheng, G. Jia, Y. Song, Y. Huang, M. Yang, J. Jia, N. Guo and H. Zhang, *J. Mater. Chem.*, 2010, **20**, 3272.

8 M. C. Das, S. C. Xiang, Z. J. Zhang and B. L. Chen, *Angew. Chem., Int. Ed.*, 2011, **50**, 10510.

9 (*a*) R. D. Rogers and K. R. Seddon, *Science*, 2003, **302**, 792; (*b*) D. S. Jacob, L. Bitton, J. Grinblat, I. Felner, Y. Koltypin and A. Gedanken, *Chem. Mater.*, 2006, **18**, 3162; (*c*) Z. Lin, D. S. Wragg, J. E. Warren and R. E. Morris, *J. Am. Chem. Soc.*, 2007, **129**, 10334; (*d*) R. E. Morris and X. Bu, *Nat. Mater.*, 2010, **2**, 353.

10 (*a*) R. Ludwig and U. Kragl, *Angew. Chem., Int. Ed.*, 2007, **46**, 6582; (*b*) L. Xu, E. Y. Choi and Y. U. Kwon, *Inorg. Chem.*, 2008, **47**, 1907; (*c*) S. M. Chen, J. Zhang and X. H. Bu, *Inorg. Chem.*, 2008, **47**, 5567.

11 (*a*) Z. Lin, A. M. Z. Slawin and R. E. Morris, *J. Am. Chem. Soc.*, 2007, **129**, 4880; (*b*) J. Zhang, S. Chen and X. Bu, *Angew. Chem., Int. Ed.*, 2008, **47**, 5434; (*c*) E. Ahmed and M. Ruck, *Angew. Chem., Int. Ed.*, 2012, **51**, 308.

12 H. M. J. Hendriks, J. M. W. L. Birker, J. V. Rijn, G. C. Verschoor and J. Reedijk, *J. Am. Chem. Soc.*, 1982, **104**, 3607.

13 (*a*) L. Cammarata, S. G. Kazarian, P. A. Salter and T. Welton, *Phys. Chem. Chem. Phys.*, 2001, **3**, 5192; (*b*) C. G. Hanke and R. M. Lynden-Bell, *J. Phys. Chem. B*, 2003, **107**, 10873.

14 (*a*) E. R. Cooper, C. D. Andrews, P. S. Wheatley, P. B. Webb, P. Wormald and R. E. Morris, *Nature*, 2004, **430**, 1012; (*b*) E. R. Parnham and R. E. Morris, *Acc. Chem. Res.*, 2007, **40**, 1005; (*c*) D. S. Wragg, A. M. Z. Slawin and R. E. Morris, *Solid State Sci.*, 2009, **11**, 411; (*d*) R. E. Morris, *Chem. Commun.*, 2009, 2990; (*e*) H. J. Ma, Z. J. Tian, R. S. Xu, B. C. Wang, Y. Wei, L. Wang, Y. P. Xu, W. P. Zhang and L. W. Lin, *J. Am. Chem. Soc.*, 2008, **130**, 8120.

15 H. S. Liu, Y. Q. Lan and S. L. Li, *Cryst. Growth Des.*, 2010, **10**, 5221.

16 (*a*) Y.-Q. Sun, J. Zhang, Y.-M. Chen and G.-Y. Yang, *Angew. Chem., Int. Ed.*, 2005, **44**, 5814; (*b*) J.-W. Cheng, S.-T. Zheng and G.-Y. Yang, *Dalton Trans.*, 2007, 4059.

17 (*a*) Y.-Q. Sun, J. Zhang and G.-Y. Yang, *Chem. Commun.*, 2006, 4700; (*b*) J.-S. Qin, D.-Y. Du, L. Chen, X.-Y. Sun, Y.-Q. Lan and Z.-M. Su, *J. Solid State Chem.*, 2011, **184**, 373.

18 T. Gunnlaugsson and J. P. Leonard, *Chem. Commun.*, 2005, 3114.

19 W. P.-W. Lai, W.-T. Wong, B. K.-F. Li and K.-W. Cheah, *New J. Chem.*, 2002, **26**, 576.

20 S. Biju, D. B. A. Raj, M. L. P. Reddy, C. K. Jayasankar, A. H. Cowley and M. Findlater, *J. Mater. Chem.*, 2009, **19**, 1425.

21 (*a*) A. M. dos Santos, F. M. B. Marques, L. D. Carlos and J. Rocha, *J. Mater. Chem.*, 2006, **16**, 3139; (*b*) X. Wang, Y. Wang, Q. Liu, Y. Li, J. H. Yu and R. R. Xu, *Inorg. Chem.*, 2012, **51**, 4779; (*c*) S. Mohapatra, S. Adhikari, H. Riju and T. K. Maji, *Inorg. Chem.*, 2012, **51**, 4891.

22 (*a*) G. M. Sheldrick, *SHELXS-97, Programs for X-ray Crystal Structure Solution*, University of Göttingen, Göttingen, Germany, 1997; (*b*) G. M. Sheldrick, *SHELXL-97, Programs for X-ray Crystal Structure Refinement*, University of Göttingen, Göttingen, Germany, 1997; (*c*) L. J. Farrugia, *WINGX, A Windows Program for Crystal Structure Analysis*, University of Glasgow, Glasgow, UK, 1988.